ISSN 0006-2979, Biochemistry (Moscow), 2010, Vol. 75, No. 7, pp. 938-943. © Pleiades Publishing, Ltd., 2010.

Isoforms of Human O-GlcNAcase Show Distinct Catalytic Efficiencies

Jing Li*, Cai-luan Huang, Lian-wen Zhang, Lin Lin, Zhong-hua Li, Fu-wu Zhang, and Peng Wang*

College of Pharmacy and State Key Laboratory of Element-Organic Chemistry, Nankai University, Tianjin 300071, China; fax: +86-22-2350-6290; E-mail: jinglink@nankai.edu.cn; pwang@nankai.edu.cn

Received March 29, 2010
Revision received May 21, 2010

Abstract—*O*-GlcNAcase (OGA) is a family 84 glycoside hydrolase catalyzing the hydrolytic cleavage of *O*-linked β-N-acetylglucosamine (*O*-GlcNAc) from serine and threonine residues of proteins. Thus far, three forms of OGA have been identified in humans. Here we optimized the expression of these isoforms in *E. coli* and characterized their kinetic properties. Using Geno 3D, we predicted that N-terminal amino acids 63-342 form the catalytic site for *O*-GlcNAc removal and characterized it. Large differences are observed in the K_m value and catalytic efficiency (k_{cat}/K_m) for the three OGA variants, though all of them displayed *O*-GlcNAc hydrolase activity. The full-length OGA had the lowest K_m value of 0.26 mM and the highest catalytic efficiency of $3.51 \cdot 10^3$. These results reveal that the N-terminal region (a.a. 1-350) of OGA contains the catalytic site for glycoside hydrolase and the C-terminal region of the coding sequence has the ability to stabilize the native three-dimensional structure and further affect substrate affinity.

DOI: 10.1134/S0006297910070175

Key words: O-GlcNAcase, isoform, substrate affinity, catalytic efficiency

O-GlcNAcylation is a newly discovered post-translational modification in cell regulation of signal transduction and now has been found in all metazoans [1-3]. So far, more than 1000 proteins (including nuclear pore proteins, cytoskeletal proteins, transcription factors, oncogenic proteins, tumor suppressor proteins, etc.) have been identified to be *O*-GlcNAcylated and these proteins are involved in many important cellular processes such as transport, transcription, cell shaping, cell signaling, and apoptosis [4-6]. Analogous to phosphorylation/dephosphorylation, the cycle of addition/removal of the sugar moiety is rapid. Emerging data have demonstrated that *O*-GlcNAcylation can play an important role in many human diseases such as type II diabetes, cancer, and neurological disorders [7-9].

Abbreviations: DTT, dithiothreitol; fOGA, full-length *O*-GlcNAcase; IPTG, isopropyl-L-thio-β-D-galactopyranoside; LB, Luria–Bertani (broth); MGEA5, meningioma expressed antigen 5; 4-MU-GlcNAc, 4-methylumbelliferyl-2-acetamido-2-deoxy-β-D-glucopyranoside; OGA, *O*-GlcNAcase; PCD, programmed cell death; sOGA, the shortest OGA; vOGA, variant of OGA.

* To whom correspondence should be addressed.

In mammals, *O*-GlcNAc cycling is regulated by two enzymes: *O*-GlcNAc transferase (OGT, EC 2.4.1.94) and *O*-GlcNAcase (OGA, EC 3.2.1.52), which are products of single genes [10, 11]. Based upon MS/MS sequencing, the human *OGA* gene has been cloned from brain [11]. Sequence alignment indicates that this gene is identical with MGEA5 (meningioma expressed antigen 5), which locates at 10q24.1-q24.3, a region associated with Alzheimer's disease [12]. The human *OGA* gene is capable of producing two separate transcripts, and each encodes a different OGA isoform. The long isoform gene consists of 16 exons and encodes a full-length protein with 916 amino acids. This full-length *O*-GlcNAcase (fOGA) is a bifunctional enzyme consisting of two domains: an N-terminal hydrolase catalytic domain belonging to glycoside hydrolase family 84 and a C-terminal domain belonging to the GCN5-related family of histone acetyltransferases [13]. The spliced transcript variant of OGA (vOGA) is the product of alternatively spliced transcript of *OGA* gene, which ignores the 5′-splicing site of intron 11 resulting in a longer exon 10 with an alternative stop codon, and it encodes a truncated protein of 677 amino acids [14]. Using cell fractionation and immunofluorescence staining, it has been shown that fOGA is primarily

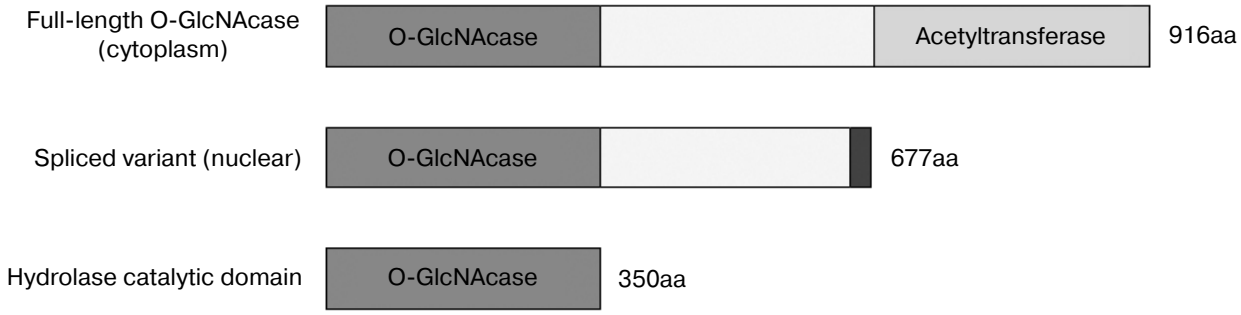

Fig. 1. Diagrammatic representation of three variants of human O-GlcNAcase. fOGA (full-length O-GlcNAcase) is the longest isoform and is composed of an N-terminal *O*-GlcNAcase domain, a linker region, and a C-terminal acetyltransferase domain. vOGA (spliced variant) contains the N-terminal *O*-GlcNAcase domain and the linker region. sOGA (hydrolase catalytic domain) is the smallest OGA consisting of N-terminal amino acids 1-350.

cytoplasmic, while vOGA is nuclear in location [15]. Based on sequence and structural information, we predicted that the N-terminal a.a. 63-342 is the catalytic site for *O*-GlcNAc removal and created another OGA variant – sOGA (the shortest OGA), which is a region corresponding to amino acids 1-350 of the amino terminus.

These three forms of OGA have identical N-terminal 1-350 amino acids, but differ in their C-terminal region (Fig. 1). Although glycoside hydrolysis activity has been reported for the three forms previously, a number of aspects about the catalysis are not clear. Is there a difference in the catalytic efficiencies of these OGAs? What is the structural basis for the glycoside hydrolase activity? What is the role of the C-terminal region in catalysis? In addition, one of the major bottlenecks for structural studies on OGAs of human origin has been the poor expression levels of the enzyme. To address these issues, we optimized the production of OGA forms using an *E. coli* expression system and then purified them. Using 4-MU-GlcNAc (4-methylumbelliferyl-2-acetamido-2-deoxy-β-D-glucopyranoside) as substrate, their steady-state kinetics were determined. The model of the catalytic domain of hOGA provides the structural basis for the hydrolytic activity of the hOGAs.

MATERIALS AND METHODS

Bacterial strains, plasmids, and materials. Human *O*-GlcNAcase cDNA (GenBank accession number AB014579) was kindly provided by Dr. Hart from the Medical School of Johns Hopkins University. *Escherichia coli* DH5α was purchased from Gibco-BRL Life Technology (USA). *Escherichia coli* BL21(DE3) was from Novagen Inc. (USA). pET-28a and pET-32a were purchased from Novagen. Restriction enzymes were obtained from Fermentas (USA). Ex Taq, Taq DNA polymerases, and T4 ligase were bought from Takara (China). 4-MU-GlcNAc (4-methylumbelliferyl-2-acetamido-2-deoxy-β-D-glucopyranoside) was purchased from Sigma Aldrich (USA). Other chemicals were of the highest grade from commercially available sources.

Cloning of fOGA, vOGA, and sOGA. Three *OGA* genes were amplified by PCR using the following primers and procedures. All primers were designed using the Primer Premier 5.0 program. Since the N-terminal 1-350 amino acids are identical, one forward primer was used for amplifying the three genes. The primer sequences were as follows: f-forward, 5′CGCGCGGCCGCGTGCAGAAGGAGAG TCAA3′ (*Not*I); f-reverse, 5′GCGCTCGAGTTACAGGCTCCGACCAAGT3′ (*Xho*I); v-reverse, 5′GCGCTCGAGAAGGGACAATATATTTGAGGAGAA3′ (*Xho*I); s-reverse, 5′GCGCTCGAGTTAATCTTCACTGTCAGTCATC3′(*Xho*I). The PCR products were subcloned in-frame into pET-28a and pET-32a between *Not*I and *Xho*I sites. The resultant constructs with *OGA* gene were subsequently transformed into *E. coli* DH5α for amplification and then into *E. coli* BL21(DE3) for protein expression. The insertion of each gene was confirmed by restriction mapping and sequencing.

Overexpression and purification of the OGAs. *Escherichia coli* BL21(DE3) transformed with the expression plasmid was grown in Luria–Bertani (LB) broth supplemented with 50 μg/ml kanamycin at 37°C at 200 rpm. Protein expression was initiated by the addition of IPTG (isopropyl-L-thio-β-D-galactopyranoside) to a final concentration of 0.01-0.5 mM when the optical density at 600 nm reached around 0.6. The cultures were further grown for 5-15 h at 16°C at 150 rpm. Cells were harvested by centrifugation and resuspended in 50 mM phosphate buffer, pH 8.0, 300 mM NaCl. The cells were sonicated using a Vibra Cell Sonifier (Scientz-IID, China) with a 19 mm-threaded probe. The sonication conditions were 10 sec per cycle (pulse on time is 2 sec, and pulse off time 8 sec), 40% output, and sonication for 30 min. Cell debris was removed by centrifugation (13,000*g*, 30 min, 4°C), and the supernatant was loaded onto a Ni^{2+}-NTA

(nickel-nitrilotriacetic acid) column (Qiagen, USA). After vigorous washing, the bound protein was eluted using 50 mM phosphate buffer, pH 8.0, 300 mM NaCl, and 300 mM imidazole. A Microcon YM-50/YM-100 microconcentrator (Millipore, USA) was used for buffer exchange and concentration. The recombinant protein was exchanged into 50 mM Tris-HCl buffer, pH 7.0, containing 1 mM dithiothreitol (DTT), 10% glycerol, and 150 mM NaCl. Protein concentration was estimated by the Bradford method [16]. The purity and apparent molecular mass were determined by SDS-PAGE [17].

Model of human OGA. A model of the catalytic domain of human OGA was generated using Geno 3D [18]. Amino acids 63-342 of human OGA matched with the primary amino acid sequence of PDB entry 2CBI, showing an identity of 34% and an *E* value of $1 \cdot 10^{-144}$. After energy minimization, a model of OGA (residues 63-342) was obtained; it had excellent geometry as judged by Ramachandran analysis.

Enzymatic assays. Assays were carried out according to the method of Macauley [19]. 4-MU-GlcNAc was used as the fluorescent substrate; 25 µl of the reaction mixture consisted of the substrate suspended in 50 mM NaH_2PO_4, 100 mM NaCl, and 0.1% BSA at pH 6.5. Assays were initiated by the addition, via syringe, of enzyme (2-6 µl), and the reaction mixture was incubated at 37°C for 4-30 min. The enzymatic reactions were quenched by the addition of 150 µl of quenching buffer (200 mM glycine, pH 10.75). A standard curve of 4-MU (4-methylumbelliferone) was obtained using a Varian Cary Eclipse fluorescence spectrophotometer 96-well plate system. Fluorescence was measured at the excitation wavelength of 368 nm and the emission wavelength of 450 nm. The produced 4-MU was determined and compared with the standard curve. All assays were performed in triplicates under identical conditions.

RESULTS

Expression of OGA. To obtain high expression, the concentration of the inducer, induction time, and induction temperature were optimized. Induction temperature is a key factor for soluble expression. When it was above 16°C, most of the protein was insoluble. So 16°C was employed for expression. Briefly, *E. coli* BL21(DE3) cells transformed with pET28a-sOGA were grown in liquid medium at 37°C until the optical density at 600 nm reached around 0.6. The effect of the concentration of IPTG and the induction time on the expression of OGA was determined by inducing individual cultures under different inducer concentrations (0.01-0.25 mM) and induction times (5-15 h). After inductions at 16°C, 10 ml of bacterial culture was centrifuged and disrupted by sonication. The supernatants of crude extracts were analyzed by 10% SDS-PAGE. The results demonstrated that His_6-tagged sOGA reached maximum soluble expression after 10 h induction with 0.05 mM IPTG (Fig. 2). Similarly, the maximum production of fOGA and vOGA was obtained when the recombinant cells were induced for 10 h with the addition of 0.25 and 0.1 mM IPTG, respectively.

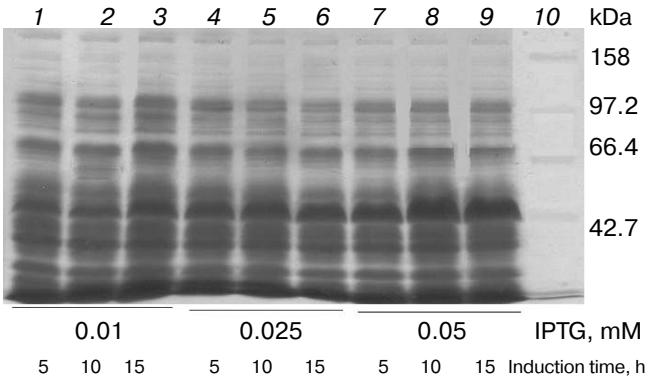

Fig. 2. Expression of His_6-tagged sOGA. Lanes: *1*) growth with 0.01 mM IPTG, 5 h; *2*) growth with 0.01 mM IPTG, 10 h; *3*) growth with 0.01 mM IPTG, 15 h; *4*) growth with 0.025 mM IPTG, 5 h; *5*) growth with 0.025 mM IPTG, 10 h; *6*) growth with 0.025 mM IPTG, 15 h; *7*) growth with 0.05 mM IPTG, 5 h; *8*) growth with 0.05 mM IPTG, 10 h; *9*) growth with 0.05 mM IPTG, 15 h; *10*) protein marker.

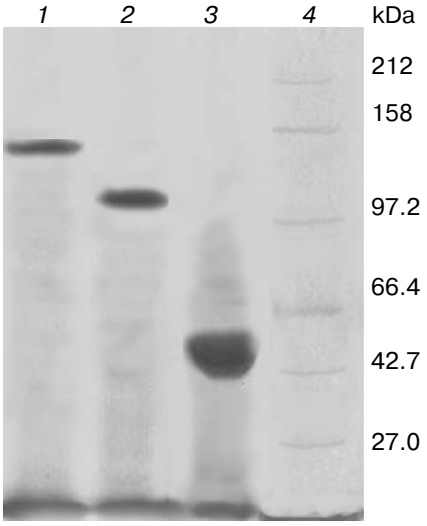

Fig. 3. SDS-PAGE of the human OGAs expressed and purified from *E. coli*. Lanes: *1*) fOGA; *2*) vOGA; *3*) sOGA; *4*) protein marker.

Production and purification of OGA. Using the optimal expression conditions, three His_6-tagged OGA genes were overexpressed and purified by Ni^{2+}-NTA chromatography. Recombinant fOGA, vOGA, and sOGA migrated at 130, 80, and 43 kDa, respectively, which is consistent with previous findings [20, 21]. Expression level of soluble

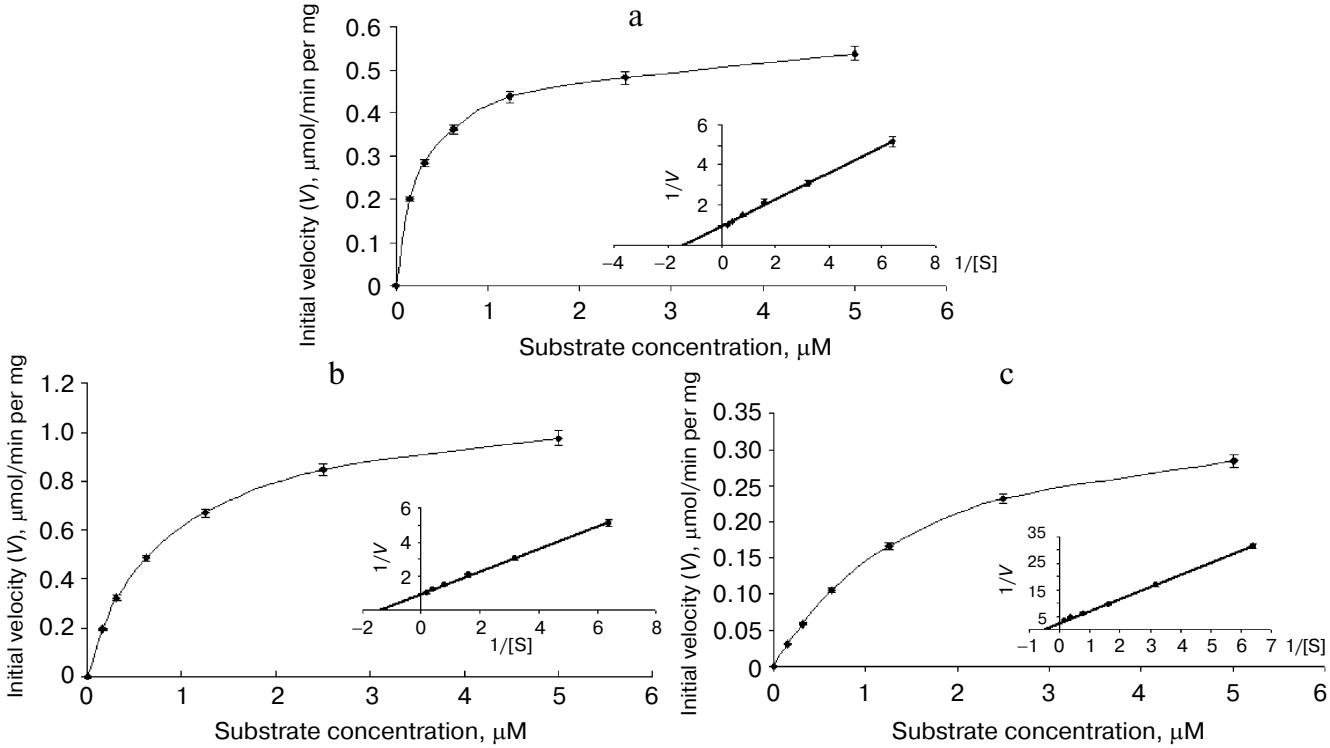

Fig. 4. Enzyme kinetics of the three His_6-tagged OGAs expressed by pET-28a(+). An activity curve and a Lineweaver–Burk plot were generated by varying concentrations of substrate (4-MU-GlcNAc). a) fOGA; b) vOGA; c) sOGA.

active OGA was 5-15 mg per liter of the culture. After Ni^{2+}-NTA affinity chromatography, the protein was more than 90% pure as judged by SDS-PAGE (Fig. 3).

Characterization of OGA. Initial velocities of the enzymatic reaction were determined by varied 4-MU-GlcNAc concentrations. Kinetic parameters including Michaelis constants (K_m), turnover numbers, and enzymatic efficiencies were calculated from Lineweaver–Burk plots (Fig. 4). The specific activity of each OGA was calculated with the methods described in "Materials and Methods".

fOGA had a K_m of 0.26 mM and a specific activity of 526 nmol/min per mg with a turnover rate of 0.9 sec^{-1}. Catalytic efficiency (k_{cat}/K_m) of fOGA was $3.5 \cdot 10^3$ $sec^{-1} \cdot M^{-1}$. Similarly, vOGA and sOGA exhibited K_m values of 0.7 and 1.84 mM and specific activities of 84 and 9 nmol/min per mg, respectively. Based on these data, the turnover numbers of vOGA and sOGA were approximately 0.11 and 0.006 sec^{-1} and catalytic efficiencies were $1.57 \cdot 10^2$ and 3.26 $sec^{-1} \cdot M^{-1}$, respectively. The kinetic values for the three OGA isoforms are summarized in the table.

Catalytic domain of human OGA is reminiscent of glucosidases. The N-terminal amino acids 63-342 of OGA could be modeled successfully using Geno 3D (Fig. 5a; see color insert). Analysis of this model revealed that the N-terminal region spanning amino acids 63-342, folds into a classical $(\alpha/\beta)_8$ TIM barrel structure commonly found in glucosidases. Three OGA forms have this identical region and all showed glucosidase hydrolysis activity in this study.

The active site pocket could be identified by superimposing the NAG-thiazoline (NGT) moiety of the bacterial *O*-GlcNAcase (PDB code 2CHN) on the modeled human OGA (Fig. 5b). Catalysis proceeds via a substrate-assisted mechanism involving the acetamido group. The acetamido group is in the vicinity of D174, which is critical for the polarization and correct orientation of the group for a nucleophilic attack at the carbonyl carbon.

Kinetic parameters of His_6-tagged recombinant human OGAs

Kinetic parameter	fOGA	vOGA	sOGA
K_m, mM	0.26 ± 0.02	0.7 ± 0.05	1.84 ± 0.01
Specific activity, nmol/min per mg	526 ± 42	84 ± 7.2	9 ± 0.7
Turnover number (k_{cat}), sec^{-1}	0.9 ± 0.07	0.11 ± 0.09	0.006 ± 0.01
Catalytic efficiency (k_{cat}/K_m), $sec^{-1} \cdot M^{-1}$	$3.51 \cdot 10^3$	$1.57 \cdot 10^2$	3.26

D175 probably assumes the role of catalytic acid. A pair of aspartates is found at similar locations in the bacterial *O*-GlcNAcase structures [22]. Y219 is within hydrogen bonding distance of the glycosidic oxygen. A tyrosine at a similar position in GH85 family of glucosidases was shown to activate a water molecule for a nucleophilic attack during the hydrolysis [23]. Residues D174, D175, and Y219 of human OGA are conserved in bacterial *O*-GlcNAcases and have been shown to be critical for catalysis [22]. The model of human OGA (amino acids 63-342) provides a structural basis for the hydrolysis activity of the three forms of hOGA.

DISCUSSION

In this study, initial steady-state enzyme kinetics for human OGAs were determined using 4-MU-GlcNAc as a substrate. fOGA has a K_m of 0.26 mM and a catalytic efficiency (k_{cat}/K_m) of $3.5 \cdot 10^3$, while vOGA and sOGA exhibited higher K_m values of 0.7 and 1.84 mM and lower catalytic efficiencies of $1.57 \cdot 10^2$ and 3.26, respectively. These results indicate that the N-terminal region harbors the catalytic site for O-GlcNAc removal, which is in agreement with many previous studies [19-21]. However, there are conflicting reports on enzymatic activity of vOGA [13, 15]. No activity was detected for vOGA expressed in either *E. coli* or COS-7 cells [15], and therefore the authors concluded that the C-terminus is necessary for O-GlcNAcase activity. We speculate that the ambiguity in the results could be a result of the expression strategy (enzyme was expressed with a thioredoxin tag) or because a less sensitive substrate (*p*NP-β-GlcNAc) was used for measuring the enzyme activity.

Thioredoxin (Trx) is an approximately 10-kDa protein fused on the N-terminus in pET-32 series to increase the solubility of recombinant proteins. To identify whether Trx impairs O-GlcNAcase catalytic activity, we subcloned three OGA isoform genes into pET-28a (with 6xHis tags only) and pET-32a (with 6xHis tags, S tag, and TRX tag), and large differences were observed in the enzyme kinetic parameters. The enzymatic activities of Trx-sOGA and Trx-vOGA were almost not detectable (data not shown). In addition, *p*NP-β-GlcNAc is a common substrate for standard OGA enzyme assay. Enzyme activity is monitored spectrophotometrically by measuring the absorbance at 400 nm of a *p*-nitrophenolate ion that is enzymatically released from *p*NP-β-GlcNAc [20]. Since the substrate undergoes only a modest change in absorbance upon cleavage, this assay is relatively insensitive. MUGlcNAc is a more sensitive fluorescence substrate for glycosidase assay; we used it to determine the kinetic parameters of the three OGA isoforms and obtained better results as expected.

O-GlcNAcylation is a highly dynamic process that is constantly responding to the extracellular environment [4, 5]. Cells under stress due to nutrient depletion or in an excessively nutrition rich environment were shown to have elevated levels of *O*-GlcNAc, which promoted cell survival [24]. Interestingly, the rate of *O*-GlcNAc cycling varies significantly for different proteins. In generally, the *O*-GlcNAc moiety of some nuclear proteins (e.g. nuclear pore proteins) is recycled slowly and has a longer half-life than that of the cytoplasmic proteins [4]. From our kinetic studies, we speculate that the difference in the half-life of the *O*-GlcNAc moiety on the proteins might be due to the different catalytic efficiencies of fOGA and vOGA.

In conclusion, we have subcloned, expressed, and characterized two isoforms of human OGA and a fragment of human OGA, designated fOGA, vOGA, and sOGA, respectively. The three recombinant forms of hOGA exhibited distinct enzymatic properties. fOGA displayed the lowest K_m value and the highest enzymatic efficiency (k_{cat}/K_m). In comparison, vOGA and sOGA, harboring a truncated C-terminal region, showed much higher K_m values and lower enzymatic efficiencies. Such differences in enzymatic efficiencies might help the OGA forms to adapt to different roles in different subcellular compartments and modulate their activities during different stages of cell development. Structural studies of human OGA support and provide structural basis for the hydrolysis activity of OGA.

The authors thank Dr. G. W. Hart from the Medical School of Johns Hopkins University for kindly providing the human O-GlcNAcase cDNA and Neil Shaw from the Institute of Biophysics, Chinese Academy of Science, and Xian-Wei Liu for kind assistance in revision of the paper.

This work was supported by the National Basic Research Program of China (973 Program, grant No. 2007CB914403).

REFERENCES

1. Henrissat, B., and Bairoch, A. (1996) *Biochem. J.*, **316**, 695-696.
2. Wells, H., Vosseller, K., and Hart, G. W. (2001) *Science*, **291**, 2376-2378.
3. Torres, C. R., and Hart, G. W. (1984) *J. Biol. Chem.*, **259**, 3308-3317.
4. Hart, G. W., Housley, M. P., and Slawson, C. (2007) *Nature*, **446**, 1017-1022.
5. Zeidan, Q., and Hart, G. W. (2010) *J. Cell. Sci.*, **123**, 13-22.
6. Zhang, F., Su, K., Yang, X., Bowe, D. B., Paterson, A. J., and Kudlow, J. E. (2003) *Cell*, **115**, 715-725.
7. Yang, X., Ongusaha, P. P., Miles, P. D., Havstad, J. C., Zhang, F., So, W. V., Kudlow, J. E., Michell, R. H., Olefsky, J. M., and Field, S. J. (2008) *Nature*, **451**, 964-969.
8. Fischer, P. M. (2008) *Nat. Chem. Biol.*, **4**, 448-449.
9. Kang, J. G., Park, S. Y., Ji, S., Jang, I., Park, S., and Kim, H. S. (2009) *J. Biol. Chem.*, **284**, 34777-34784.

10. Lubas, W. A., Frank, D. W., Krause, M., and Hanover, J. A. (1997) *J. Biol. Chem.*, **272**, 9316-9324.
11. Gao, Y., Wells, L., Comer, F. I., Parker, G. J., and Hart, G. W. (2001) *J. Biol. Chem.*, **276**, 9838-9845.
12. Bertram, L., Blacker, D., Mullin, K., Keeney, D., Jones, J., Basu, S., Yhu, S., and Tanzi, R. E. (2000) *Science*, **290**, 2302-2303.
13. Schultz, J., and Pils, B. (2002) *FEBS Lett.*, **529**, 179-182.
14. Comtesse, N., Maldener, E., and Meese, E. (2001) *Biochem. Biophys. Res. Commun.*, **283**, 634-640.
15. Wells, L., Gao, Y., Mahoney, J. A., Vosseller, K., Chen, C., Rosen, A., and Hart, G. W. (2002) *J. Biol. Chem.*, **277**, 1755-1761.
16. Bradford, M. M. (1976) *Anal. Biochem.*, **72**, 248-254.
17. Laemmli, U. K. (1970) *Nature*, **227**, 680-685.
18. Christophe, C., Martin, J., Gilbert, D., and Christophe, G. (2002) *Bioinformatics*, **18**, 213-214.
19. Macauley, M. S., Whitworth, G. E., Debowski, A. W., Chin, D., and Vocadlo, D. J. (2005) *J. Biol. Chem.*, **280**, 25313-25322.
20. Kim, E. J., Kang, D. O., Love, D. C., and Hanover, J. A. (2006) *Carbohydr. Res.*, **341**, 971-982.
21. Cuetinbasu, N., Macauley, M. S., Stubbs, K. A., Drapala, R., and Vocadlo, D. J. (2006) *Biochemistry*, **45**, 3835-3844.
22. Dennis, R. J., Taylor, E. J., Macauley, M. S., Stubbs, K. A., Turkenburg, J. P., Hart, S. J., Black, G. N., Vocadlo, D. J., and Davies, G. J. (2006) *Nat. Chem. Biol.*, 13365-13371.
23. Yin, J., Li, L., Shaw, N., Li, Y., Song, J. K., Zhang, W., Xia, C. F., Zhang, R. G., Joachimiak, A., Zhang, H. C., Wang, L. X., Liu, Z. J., and Wang, P. (2009) *PLoS ONE*, **4**, e4658.
24. Zachara, N. E., and Hart, G. W. (2004) *Biochim. Biophys. Acta*, **1673**, 13-28.